

Sensing of indoor temperature using acoustic tomography: Optimizing inaccurate loudspeaker and microphone xyz -coordinates

Cherif Othmani*, Sebastian Merchel, M. Ercan Altinsoy

Chair of Acoustics and Haptic Engineering, Dresden University of Technology, 01062 Dresden, Germany,

*E-Mail: cherif.othmani@tu-dresden.de, othmanicheriffss@gmail.com

Introduction

Acoustic travel-time TOMography (ATOM) technique is presented as a possibility for remote sensing of indoor air temperature field [1-3]. Here, measured time-of-flight (ToF) values of sound signals between transmitter (e.g. loudspeaker) and receiver (microphone) are used as input data to derive spatially averaged quantities inside a room. We can benefit not only from the direct ray path between the transceiver [4] but also from the generated early reflections, in order to minimize the number of used devices [2]. Usually, the coordinates of transceiver are known, however, practical constraints often prevent the accurate access of these coordinates, which can have an impact on the measurement accuracy. In the references [2, 3], the distance between the loudspeaker and the microphone was adjusted to take into account the impact of the inaccurate positions of the transceiver, and thus to minimize the measurement discrepancy. We "steal" this motivating idea from the work of Othmani et al. [2] and Dokhanchi et al. [3]. In contrast to references [2, 3], we calibrate the ATOM setup without adjusting the distance between the loudspeaker and microphone in order to take into account the impact of the inaccurate positions of the transceiver. Thus, in the present work, we show that such an adjustment of distance between loudspeaker and microphone [2, 3] is not the only usable method, where a new robust numerical method can be developed and applied to predict the approximate correct xyz -coordinates of the transceiver. The numerical procedure of this approach is as follows: collect all updated coordinates of the transceiver, where the calculated speed and measured speed of the direct ray path coincide (with an uncertainty of no more than 0.1 m/s). Then, we can calculate the ToF of early reflections under the different collected updated coordinates that should correspond to those obtained by the image source model (ISM). Subsequently, we can exclude the coordinates who do not fit the above-mentioned requirements from the total number. This numerical method offers multiple updated coordinates of the transceiver that may be used for gaining more comprehensive information about the ToF of early reflections peaks in RIR. Our hope is that the present idea will provide a good entry point for those wishing to learn much more, and inspire new methods to improve the measurement accuracy.

Theoretical basis and experimental setup of ATOM technique

Theoretical basis

Laplace's equation of sound speed with respect to the adiabatic conditions satisfies the following equation [1, 2].

$$c = \sqrt{\gamma \times R_s \times T} \quad (1)$$

where T is the gas temperature. $R_s = 287.058 \text{ Jkg}^{-1}\text{K}^{-1}$ and $\gamma = 1.40$ denote the specific constant for gas (dry air) and the ratio of specific heat capacities at constant pressure and volume for gas, respectively [1-3]. Moreover, it is worth mentioning that the dry air in the room can be considered as an ideal gas. Thus, the temperature can be easily derived out from Eq. (1) as:

$$T = \frac{c^2}{\gamma \times R_s} = \frac{1}{s^2 \times \gamma \times R_s} \quad (2)$$

where s denotes the slowness (i.e. inverse of sound velocity c (m/s)). Considering the reasoning from the ATOM setup, if we correctly measure the ToF of early reflections in the box impulse response, we can derive the sound velocity c by applying the following equation [1-3]:

$$\text{ToF}_i = \int_{\text{ray}=l_i} \frac{dl_i}{c(r)} \quad (3)$$

ToF_i denotes the ToF for i^{th} ray path along the sound propagation ray paths (l_i). The next subsection summarizes the still open question related to the used experiment ATOM setup to measure the ToF in Eq. (3).

Indoor acoustic tomography array

As shown in Fig. 1, we consider a plexiglass box (1.33 m \times 1.0 m \times 1.27 m) for the indoor acoustic tomography array [2]. Note that the x , y and z dimensions of the box are not arbitrarily chosen, but have already been used by Barth and Raabe [4] for a frame to reconstruct the indoor temperature using only the direct ray paths. In reference [2], we show that this plexiglass box is capable of generating several early reflections. We can take advantage of these early reflections by avoiding the use of multiple loudspeakers and microphones (as in the work of Barth and Raabe [4]), and therefore reducing the operational costs. In this regard, one *W3-315E* loudspeaker and one omnidirectional *MK 301E* microphone were positioned in the box at optimal positions: $OP \in \{s[0.2 \ 0.7 \ 0.9], r[1.1 \ 0.2 \ 0.5]\}$ [2]. For a more detailed background on the implemented numerical method for predicting the optimal positions of the transmitter and receiver, we recommend reading the reference [2]. However, it is important to note that we estimate the ToF of the early reflections, considering the first-, second-, and third-orders. The rate of coverage ray-paths of the above-mentioned optimal position can be numerically verified using the visualization of the image sound source model (ISM) [2], as shown in Fig. 2. It can be seen that the number of the ray-paths has decreased from 60 ray paths [2] to 21 ray paths, when considering the angle directivity of the loudspeaker ($\pm 50^\circ$). Although considering the radiation angle of the loudspeaker significantly reduces

the number of generated ray paths, the ISM visualization (Fig. 2) suggests that the tomography area may be perfectly covered under the above-mentioned optimal position.

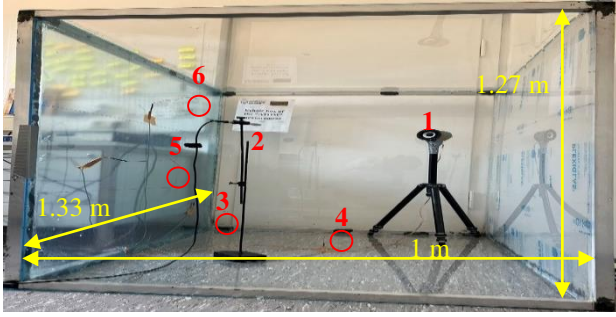


Figure 1. Tomography area: a plexiglass box (1.33 m × 1.0 m × 1.27 m). Here, (1): *W3-315E* loudspeaker, (2): *MK 301E*, (3-6): NTC- thermistors (adapted from Reference [2]).

In addition to the transceiver, the ATOM layout includes an RME Fireface (with 192 kHz), a computer with MATLAB, signal converter and power amplifier. On the other hand, 4 NTC thermistors are used as a benchmark, where they are placed in 4 different positions inside the box (see points 3-6 in Fig. 1). Moreover, the swept-sine signal (2000 Hz-12000 Hz) [2, 5] is presented as an excitation signal. For more details on the advantages of the swept-sine signal, we refer the reader to the both references [2, 5].

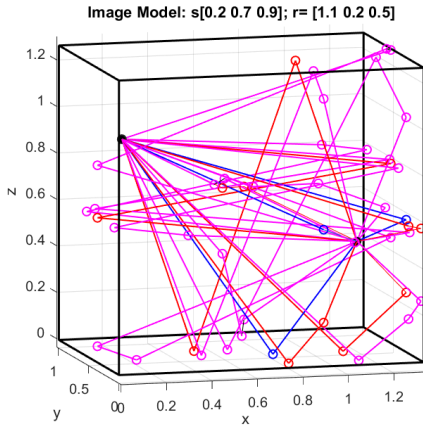


Figure 2. ISM visualization of the coverage box considering the first- (blue color), second- (red color) and third-orders (magenta color) at the sound source angle of $\pm 50^\circ$. Here, the optimal position is $OP \in \{s[0.2 \ 0.7 \ 0.9], r[1.1 \ 0.2 \ 0.5]\}$ [2].

The measured impulse response of the plexiglass box (1.33 m × 1.0 m × 1.27 m) and the detected ToF are shown in the next subsection.

Measured impulse response and estimation the ToF

For an impulse response $h(t)$ within any linear time-invariant (LTI) system, we consider an input $x(t)$, where output $y(t)$ convolutive problem as [3]:

$$y[t] = h[t] * x[t] \tag{4}$$

Here, "*" is convolution. From here, we can write $y[t]$ as [3]:

$$y[t] = \sum_{k=-\infty}^{\infty} h[k]x[t-k] \tag{5}$$

k is the dummy variable of the summation index.

We go through the measured impulse response $h(t)$, and then explain how we can predict the desired ToF of early reflections. First, cross-correlation (CC) technique between transmitted swept-sine signal and recorded signal has been used to estimate ToF for the direct ray path. For a complete picture and more details on the CC technique, we refer the reader to references [1-3]. Then, we can apply the peak detection approach for estimating the ToF of the different generated early reflections [2, 3]. This step considers several complicated scenarios as explained clearly by Othmani et al. [2] and Dokhanchi et al. [3]. A further improvement in terms of ToF detection can be achieved by using the ISM simulated ToF of early reflections (Fig. 3) as markers to accurately estimate the correct and desired peaks from the measured impulse response (the measured $h(t)$ is not included here just for brevity). It is worth mentioning that the first-, second- and third-order reflections under the optimal position (OP) and at the loudspeaker radiation angle of $\pm 50^\circ$ are explicitly considered. Thus, creating a short analysis window around the measured peaks can be beneficial in this scenario, where each window length is deeply related to the distributions of the simulated ToF of early reflection peaks (Fig. 3).

We move to the backward ATOM problem, where the ToF of the early reflection peaks collected above can be used as input data for an inverse algorithm to estimate the interior temperature distributions within the plexiglas box (1.33 m × 1.0 m × 1.27 m). In this study, simultaneous iterations reconstruction technique (SIRT) is applied to achieve this goal. A more detailed discussion of the SIRT procedure is given in references [1-3].

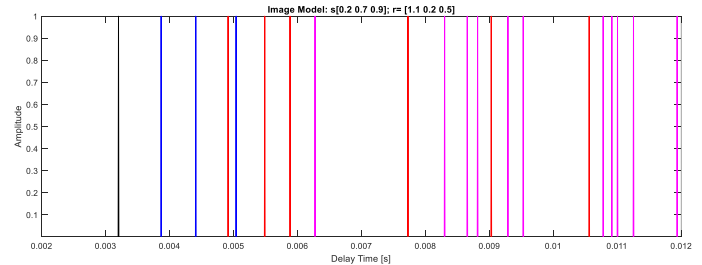


Figure 3. ISM simulated ToF of early reflections peaks under the optimal position and at the source angle of 50° , (black color), direct sound ray; (blue color), first order reflections; (red color), second order reflections; (magenta color), third order reflections.

Optimizing the inaccurate coordinates of transceiver: a new numerical approach

One of the recent works, by Dokhanchi et al. [3], proposes the adjustment of the distance between the transmitter and the receiver to take into account the inaccurate positions of the transceiver and thus minimize the measurement discrepancy. Instead, we propose a new numerical approach for the estimation of an accurate x -, y - and z -coordinate of the transceiver, which can be an alternative pre-eminent to handle the above-mentioned problem. This numerical method enables us to recover the exact transmitter/receiver coordinates based on calculated speed (c^{cal}) and measured speed (c^{meas}) of the direct ray path. This target can be

achieved by expanding the x -, y -, and z -coordinates margin of the transmitter and receiver in both negative and positive direction, which given as:

$$\forall_{source} = \left\{ \begin{array}{l} (s_x, s_y, s_z) | s_x^{\min} \leq s_x \leq s_x^{\max}, \\ s_y^{\min} \leq s_y \leq s_y^{\max}, s_z^{\min} \leq s_z \leq s_z^{\max} \end{array} \right\} \quad (6a)$$

$$\forall_{receiver} = \left\{ \begin{array}{l} (r_x, r_y, r_z) | r_x^{\min} \leq r_x \leq r_x^{\max}, \\ r_y^{\min} \leq r_y \leq r_y^{\max}, r_z^{\min} \leq r_z \leq r_z^{\max} \end{array} \right\} \quad (6b)$$

where, s_x, s_y, s_z and r_x, r_y, r_z are the updated xyz -coordinates of loudspeaker and microphone, respectively. However, $s_x^{\min} = s_y^{\min} = s_z^{\min} = s - \alpha$, $s_x^{\max} = s_y^{\max} = s_z^{\max} = s + \alpha$,

$r_x^{\min} = r_y^{\min} = r_z^{\min} = r - \alpha$ and $r_x^{\max} = r_y^{\max} = r_z^{\max} = r + \alpha$. Here, α is set at 1 mm, and s and r denote the original xyz -coordinates of source and receiver, respectively ($OP \in \{s[0.2 \ 0.7 \ 0.9], r[1.1 \ 0.2 \ 0.5]\}$). According to Eq. (6) and in order to estimate the total possible updated xyz -coordinates, $s_x / s_y / s_z$ and $r_x / r_y / r_z$ coordinates margin of source and receiver, respectively, are subdivided into multiple bins. Then, we should identify the desired threshold (Δ) between the calculated speed (c^{cal}) and measured speed (c^{meas}) of the direct ray path. In this numerical procedure, any difference between c^{cal} and c^{meas} less than 0.1m/s can be considered a possible acceptable threshold. Accordingly, to obtain the desired xyz -coordinates of source and receiver that fit the above requirements, the set Ω can be written as:

$$\Omega_s \in \arg \min_{\{(s_x, s_y, s_z)\}} \left\{ \mathbb{N}_s \left(\begin{array}{l} |c^{cal}(s_x, s_y, s_z) - c^{meas}(s_x, s_y, s_z)| \leq \Delta \end{array} \right) \right\} \quad (7a)$$

$$\Omega_r \in \arg \min_{\{(r_x, r_y, r_z)\}} \left\{ \mathbb{N}_r \left(\begin{array}{l} |c^{cal}(r_x, r_y, r_z) - c^{meas}(r_x, r_y, r_z)| \leq \Delta \end{array} \right) \right\} \quad (7b)$$

where, \mathbb{N}_s and \mathbb{N}_r function as an indicators:

$$\mathbb{N}_s = \begin{cases} 0 & \text{if } \left| \begin{array}{l} c^{cal}(s_x, s_y, s_z) \\ -c^{meas}(s_x, s_y, s_z) \end{array} \right| > \Delta \\ 1 & \text{if } \left| \begin{array}{l} c^{cal}(s_x, s_y, s_z) \\ -c^{meas}(s_x, s_y, s_z) \end{array} \right| \leq \Delta \end{cases} \quad (8a)$$

$$\mathbb{N}_r = \begin{cases} 0 & \text{if } \left| \begin{array}{l} c^{cal}(r_x, r_y, r_z) \\ -c^{meas}(r_x, r_y, r_z) \end{array} \right| > \Delta \\ 1 & \text{if } \left| \begin{array}{l} c^{cal}(r_x, r_y, r_z) \\ -c^{meas}(r_x, r_y, r_z) \end{array} \right| \leq \Delta \end{cases} \quad (8b)$$

Once we incorporate the both indicators \mathbb{N}_r and \mathbb{N}_s in the numerical procedure, we can collect the different desired xyz -coordinates of source and receiver which fit the above-mentioned requirements. Accordingly, a total of 350 updated x -, y - and z -coordinates of the source and the receiver have been predicted by the proposed numerical method within the above identified range of 1 mm ($\alpha = 1$ mm). It is worth noting that the updated speed of sound at these 350 coordinates is in the range of 344.1 m/s to 344.2 m/s. If the ToF of the direct ray path of these 350 updated coordinates satisfies the above-identified threshold (Δ),

"how about the corresponding ToF of early reflection peaks?". In order to select the correct desired updated x -, y - and z -coordinates of the source and receiver, the answer to this critical question can be helpful.

The next step is a simple check of the measured ToF (τ^{meas}) and the iterated ToF (τ^{iter}) of the different early reflections under the updated 350 coordinates of source and receiver. Here, it is worth noting that the Simultaneous Iterative Reconstruction Technique (SIRT) algorithm [1, 2] requires M iterations to reach the desired solution, thus came the so-called iterated ToF (τ^{iter}). We refer the reader to the review paper by Othmani et al. [1] for more details on the iteration procedure using the SIRT method. On the other hand, we can expect the desired coordinates to maintain the 21 ray paths that generated by the original coordinate ($OP \in \{s[0.2 \ 0.7 \ 0.9], r[1.1 \ 0.2 \ 0.5]\}$), with the τ^{meas} and τ^{iter} of early reflections coincide. Surprisingly, we show that only 19 of the above 350 updated coordinates match these requirements of the ToF of early reflections. However, the remaining 331 coordinates either produced a smaller number of the desired ray paths of early reflections (21 ray paths) or they did not meet the ToF requirement of early reflections. Moreover, some coordinates from the 331 cases did not meet the requirements of optimal source and receiver positions, where it can happen that some ray paths overlap [2]. Actually, this overlap between the different ray paths has a significant negative effect on the measurement accuracy. It is worth mentioning that this paper considers and discusses the above desired 19 cases (cases 1 to 19 in Table 1) and one case from 331 coordinates (case 20 in Table 1).

Table 1. Details on the coordinates of source and receiver.

Case number	Source coordinates (x,y,z)	Receiver coordinates (x,y,z)	ΔT ($^{\circ}C$)
1	[0.199 0.699 0.899]	[1.099 0.199 0.5005]	0.16
2	[0.199 0.699 0.899]	[1.099 0.199 0.5]	0.24
3	[0.199 0.699 0.899]	[1.0995 0.199 0.501]	0.26
4	[0.199 0.699 0.899]	[1.0995 0.1995 0.5005]	0.26
5	[0.199 0.699 0.899]	[1.0995 0.201 0.499]	0.2
6	[0.199 0.699 0.899]	[1.1 0.2005 0.5]	0.28
7	[0.199 0.699 0.899]	[1.1 0.2005 0.501]	0.17
8	[0.199 0.699 0.899]	[1.1005 0.201 0.5005]	0.31
9	[0.199 0.699 0.899]	[1.1005 0.201 0.501]	0.24
10	[0.199 0.699 0.8995]	[1.099 0.199 0.5005]	0.22
11	[0.199 0.699 0.8995]	[1.099 0.199 0.501]	0.17
12	[0.199 0.699 0.8995]	[1.099 0.1995 0.5]	0.22
13	[0.199 0.699 0.8995]	[1.099 0.2005 0.499]	0.19
14	[0.199 0.699 0.9005]	[1.0995 0.2005 0.5005]	0.32
15	[0.199 0.6995 0.8995]	[1.099 0.2005 0.499]	0.31
16	[0.199 0.6995 0.901]	[1.099 0.2005 0.501]	0.19
17	[0.199 0.7 0.8995]	[1.099 0.2005 0.5]	0.26
18	[0.1995 0.699 0.899]	[1.0995 0.199 0.5]	0.26
19	[0.1995 0.699 0.899]	[1.1005 0.2005 0.501]	0.17
20	[0.195 0.699 0.901]	[1.099 0.2005 0.499]	8.09

Analysis of results

Fig. 4 shows the 3D reconstructed temperature for cases 1, 2, 8 and 20. It is worth noting that the 3D reconstructed temperature for the remaining cases are not included here just for brevity. For more details on the max error on temperature in these cases, we refer the reader to Table 1.

Here, the maximum temperature error can be defined as $\Delta T(^{\circ}\text{C}) = (\max|T^{ATOM} - T^{NTC}|)$, where $T^{NTC} = 21.5^{\circ}\text{C}$ and T^{ATOM} are the measured value of temperature using NTC-thermistor and ATOM technique, respectively. First, the 3D dimensional view of temperature distribution under cases 1, 2 and 8 is illustrated in Figs. 4 (a), (b) and (c), respectively. It can be seen that the relative error on temperature (ΔT) are approximately 0.16, 0.24 and 0.31 $^{\circ}\text{C}$ (max), respectively. Further details are reported in Table 1. Next, it can be seen that the reconstructed field of temperature distribution within the 8 voxels under case 20 is unsatisfying to the different NTC-thermistors measurement of 21.5°C . The max error on temperature under this case is 8.09°C (see Fig. 4 (d) and Table 1).

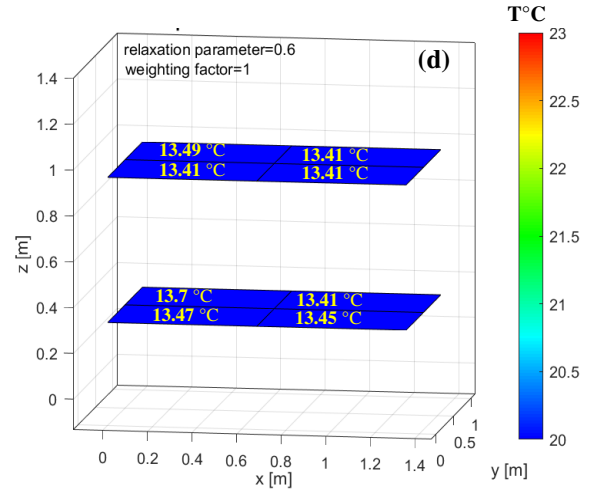
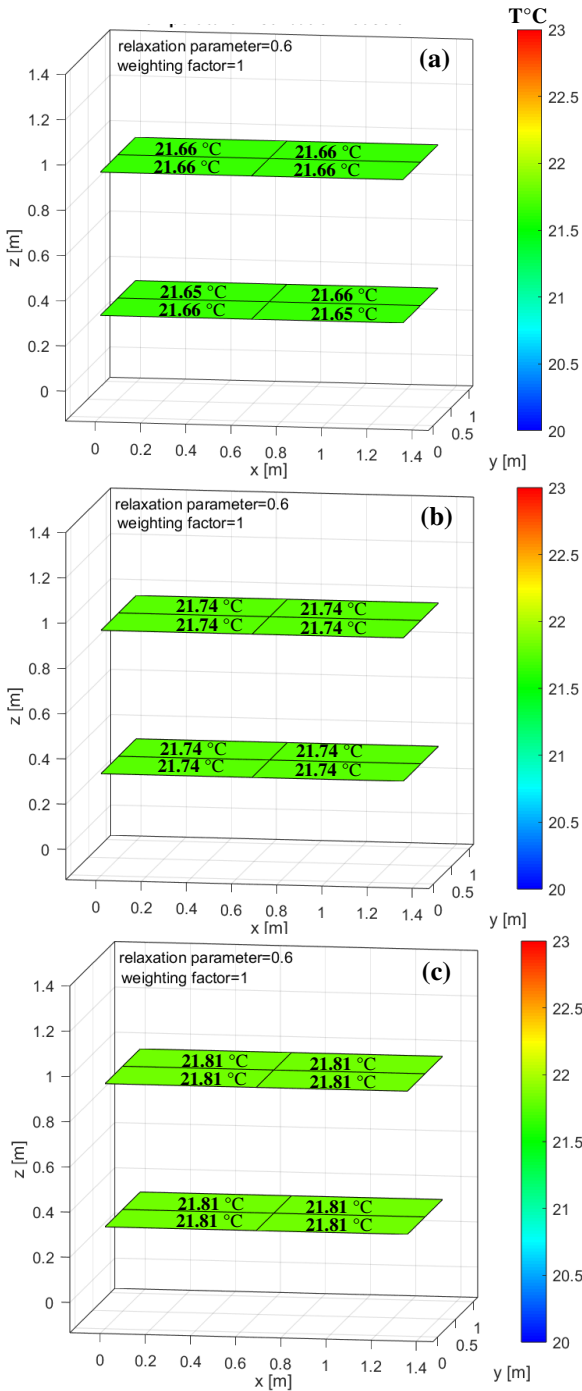


Figure 4. 3D distribution of reconstructed indoor temperature: (a), case 1; (b), case 2; (c), case 8; (d), case 20.

Conclusions

We have proposed a new robust and accurate calibration method to predict the approximate correct x -, y - and z -coordinates of the transceiver based on the calculated speed and measured speed of the direct ray path. The method exploits the calculated ToF of early reflections peaks provided by ISM. Accordingly, we have shown how the updated coordinates of source and receiver may be used to better reconstruct indoor temperature using ATOM system.

Acknowledgments

This research was funded by the Deutsche Forschungsgemeinschaft (DFG - German Research Foundation) under grant number 465591632. Additionally, we highly appreciate the scientific collaboration with our project partners at the Department of Building Physics, Bauhaus-University Weimar.

References

- [1] C. Othmani, N. S. Dokhanchi, S. Merchel, A. Vogel, M. E. Altinsoy, C. Voelker, F. Takali, Acoustic tomographic reconstruction of temperature and flow fields with focus on atmosphere and enclosed spaces: A review, *Applied Thermal Engineering* 223 (2023) 119953.
- [2] C. Othmani, S. Merchel, M. E. Altinsoy, F. Takali, Acoustic Travel-Time TOMography technique to reconstruct the indoor temperature: how to improve the field reconstruction quality?, *IEEE Transactions on instrumentation and measurement*, 73 (2024) 6500214.
- [3] N. S. Dokhanchi, J. Arnold, A. Vogel, C. Voelker, Measurement of indoor air temperature distribution using acoustic travel-time tomography: Optimization of transducers location and sound-ray coverage of the room, *Measurement* 164 (2020) 107934.
- [4] M. Barth, A. Raabe, Acoustic tomographic imaging of temperature and flow fields in air, *Measurement Science and Technology* 22 (2011) 035102.
- [5] A. Farina, Advancements in impulse response measurements by sine sweep, In *Proceedings of the 112nd AES Convention, Vienna, Austria, (2007) 5–8.*